Biaxial stress relaxation of semilunar heart valve leaflets during simulated collagen catabolism: Effects of collagenase concentration and equibiaxial strain state

Siyao Huang and Hsiao-Ying Shadow Huang

Abstract

Heart valve leaflet collagen turnover and remodeling are innate to physiological homeostasis; valvular interstitial cells routinely catabolize damaged collagen and affect repair. Moreover, evidence indicates that leaflets can adapt to altered physiological (e.g. pregnancy) and pathological (e.g. hypertension) mechanical load states, tuning collagen structure and composition to changes in pressure and flow. However, while valvular interstitial cell-secreted matrix metalloproteinases are considered the primary effectors of collagen catabolism, the mechanisms by which damaged collagen fibers are selectively degraded remain unclear. Growing evidence suggests that the collagen fiber strain state plays a key role, with the strain-dependent configuration of the collagen molecules either masking or presenting proteolytic sites, thereby protecting or accelerating collagen proteolysis. In this study, the effects of equibiaxial strain state on collagen catabolism were investigated in porcine aortic valve and pulmonary valve tissues. Bacterial collagenase (0.2 and 0.5 mg/mL) was utilized to simulate endogenous matrix metalloproteinases, and biaxial stress relaxation and biochemical collagen concentration served as functional and compositional measures of collagen catabolism, respectively. At a collagenase concentration of 0.5 mg/mL, increasing the equibiaxial strain imposed during stress relaxation (0%, 37.5%, and 50%) yielded significantly lower median collagen concentrations in the aortic valve ($p = 0.0231$) and pulmonary valve ($p = 0.0183$), suggesting that relatively large strain magnitudes may enhance collagen catabolism. Collagen concentration decreases were paralleled by trends of accelerated normalized stress relaxation rate with equibiaxial strain in aortic valve tissues. Collectively, these in vitro results indicate that biaxial strain state is capable of affecting the susceptibility of valvular collagens to catabolism, providing a basis for further investigation of how such phenomena may manifest at different strain magnitudes or in vivo.

Introduction

Aortic heart valve leaflets are at once structurally elegant and mechanically robust, measuring a mere 300–700 μm thick, but capable of bearing 80 mmHg pressure gradients,[1] flexural change in curvature of $0.6 \, \text{mm}^{-1}$,[2–4] and $> 20 \, \text{dyne/cm}^2$ fluid shear stresses.[5,6] These structural–mechanical functions are accomplished $\sim 3 \times 10^9$ times during a human lifespan through an anisotropic, trilaminar, and hierarchical extracellular matrix (ECM) structure of collagens, proteoglycans, and elastin—but not without withstanding damage and affecting repair. Valvular collagens are susceptible to fatigue[7] and turnover about every

8 weeks (in rats[8]). Indeed, evidenced by the relatively limited durability of nonviable bioprosthetic heart valves,[9] the lifelong durability of healthy heart valve leaflets derives not from their ability to bear load but from their ability to *transmit* load into their

Department of Mechanical & Aerospace Engineering, North Carolina State University, Raleigh, NC, USA

Corresponding author:
Hsiao-Ying Shadow Huang, Department of Mechanical & Aerospace Engineering, North Carolina State University, R3158 Engineering Building 3, Campus Box 7910, 911 Oval Drive, Raleigh, NC 27695, USA.
Email: hshuang@ncsu.edu

collagenous interstitium, eliciting repair by their resident valvular interstitial cells (VICs).

Distributed throughout the fibrosa, spongiosa, and ventricularis layers of the leaflets, VICs are capable of sensing and responding to forces communicated through the ECM.[1,10–13] Healthy leaflets imply homeostasis, with subpopulations of VICs catabolizing damaged collagen and the same or other VICs mediating de novo collagen synthesis.[8,13,14] By contrast, disruption, depletion, or excess accretions of collagens are hallmarks of various valvular diseases,[15–21] likely manifesting as causes and effects of disrupted mechanotransduction across the macro to micro length scales. These two sides of the remodeling coin beg the question: what are the signals that instruct VICs to turnover collagen? Nonphysiological stresses and strains are capable of eliciting VIC secretion of collagenolytic matrix metalloproteinases (MMPs),[22,23] such as in the high stress vicinity of calcific nodules,[24] and likely mediated through changes in VIC deformation.[10,11,25–28] However, how then would VIC-secreted MMPs differentiate damaged and denatured collagen from functional, structurally load-bearing fibers?

The answer may lie in load bearing itself. In 1977, Huang and Yannas[29] demonstrated that the susceptibility of bovine tendon-derived collagen to enzymatic cleavage can depend on the strain state of the fiber. Studies by Nabeshima et al.,[30] and more recently the laboratory of Ruberti and colleagues,[31–38] support the hypothesis that collagen exhibits "mechanochemical switches." Collagen fiber strain may effectively block proteolytic sites through triple-helix structural rearrangement,[32,34] thereby conferring resistance to degradation, leaving unloaded fibers selectively susceptible to collagenases and MMPs.[36] Conceptually, this paradigm could potentially explain how molecular-level collagen damage elicits selective collagen fiber remodeling and has broader implications for developmental tissue growth, physiological load adaption, and pathological degeneration.[31,38] Nevertheless, it remains unclear how such strain-dependent phenomena may manifest in heart valve leaflets, which exhibit nonorthogonal collagen fiber orientation distributions and complex loading states.

Unlike tendons, heart valve leaflets exhibit relatively broad planar distributions of collagen fiber angular orientation[39] and circumferential and radial physiologic loading components, a stress–strain state amenable to simulation by biaxial mechanical testers.[40] Together, these structural and physiological loading properties confer slack and induce fiber rotations, factors which collectively confound direct relationships between macro-scale, tissue-level strain, and the state of strain within individual collagen fibers.[7,41] Ruberti and colleagues[33,37,38] have leveraged the orthogonal collagen fiber orientations of corneal tissue to demonstrate selective degradation of intrinsic "control fibers" perpendicular to the loading axis. To date, however, the closest evidence for collagen fiber strain-state-dependent

catabolism directly relevant to heart valves comes from studies of bovine pericardium,[41] a tissue routinely utilized in the fabrication of chemically cross-linked bioprosthetic heart valves.

To understand whether physiologically relevant biaxial strain states are capable of influencing the susceptibility of valvular collagens to catabolism, in this study, stress relaxation studies similar to those of Huang and Yannas[29] were conducted on porcine aortic valve (AV) and pulmonary valve (PV) leaflet tissues. Similar to recent work by Rodriguez and Masters[42] in the context of valvular calcification, bacterial collagenase was utilized to simulate the effects of endogenous MMPs involved in physiologic valvular collagen remodeling. Stress relaxation tests were conducted under different equibiaxial strain magnitudes (37.5% and 50%) and collagenase concentrations (0.2 and 0.5 mg/mL). Toward corroborating stress relaxation mechanical data, residual collagen concentration was measured biochemically.[40]

Materials and methods

Preparation of tissue specimens and collagenase solutions

Nine porcine hearts (mixed breed sows, from 8-month to 1-year old) were retrieved from the Nahunta Pork Center (Pikeville, NC) and returned to the laboratory in a bag of ice-cold Hank's balanced salt solution (HBSS; Lonza, Walkersville, MD) on ice within 60 min. Sows were slaughtered by bleeding after being rendered unconscious by a captive bolt stunner. A total of 27 AV leaflets and 27 PV leaflets were collectively excised from the aortas and pulmonary arteries, respectively. Specifically, the AV and PV were dissected from each heart, and the leaflets were removed from their respective roots. The removal was completed by cutting axially along the aorta and pulmonary artery toward the heart until the valves were reached. Each leaflet was then stretched out and held taut while being cut against the wall of the artery. Square specimens (10 mm × 10 mm) were dissected from each leaflet such that specimen axes corresponded with the circumferential and radial directions of the leaflets.[40] Leaflet specimens were immediately immersed in 37 °C HBSS. Collagenase solutions (i.e. 0.2 and 0.5 mg/mL) were prepared by dissolving collagenase, type 2 derived from *Clostridium histolyticum* (Cat. # LS004176; Worthington Biochemical Corp., Lakewood Township, NJ) in HBSS. Collagenase solutions were refrigerated at 4 °C prior to use.

Biaxial tissue tester system

Our laboratory's biaxial tensile mechanical testing system and protocols have been described in detail.[40] In brief, a biaxial tissue tester (BioTester 5000; CellScale, Waterloo, ON, Canada) equipped with motors and

load cells (500 mN) capable of independently actuating and monitoring two perpendicular axes was used for applying and measuring tissue loads and displacements. Four "BioRake" grips were utilized to provide uniform load distribution across a 4 mm length of each of the four edges of a square tissue specimen. Measured load and displacement data were exported and post-processed using Microsoft Excel to analyze and plot stress–strain data and to calculate tissue mechanical properties.

Stress relaxation experiments

A total of n = 18 AV and n = 18 PV specimens were assigned to the collagenase-treated (experimental) group, and n = 6 AV and n = 6 PV specimens were assigned to the untreated (control) group (leaving n = 3 AV and n = 3 PV specimens for zero strain, no collagenase collagen assay samples). Four experimental conditions were tested (n = 3 AV and n = 3 PV each), comprising two collagenase concentrations (i.e. 0.2 and 0.5 mg/mL) at each of two equibiaxial strain magnitudes (i.e. 37.5% and 50%). The two control conditions (n = 3 AV and n = 3 PV each) comprised 37.5% and 50% equibiaxial strain in the absence of collagenase. Of note, equibiaxial strain was utilized to minimize collagen fiber rotations, thereby largely preserving the original collagen fiber orientations.[43]

Square 10 × 10-mm tissue specimens dissected as described above were mounted such that the first and second axes of the BioTester corresponded with the circumferential and radial directions of the valve leaflet, respectively. To mitigate tissue tearing prior to stress relaxation, 10 preconditioning cycles (10% strain) were applied at a strain rate of 2.5% per second. The preconditioning cycles were followed by a 30-s rest period. Finally, the target strain magnitude was reached via a sequence of alternating 5-s stretch, 5-s hold steps (three steps of 12.5% strain each to reach 37.5%; four steps of 12.5% strain each to reach 50%).[44] The time at which the strain reached 37.5% (or 50%) was designated as time 0 (i.e. t = 0 s), and the specimen was subsequently held 10,000 s.[45,46] For each of the experimental conditions, the specimens were immersed in 37 °C HBSS for the first 3000 s, following which the HBSS was replaced with collagenase solution using a serological pipette and pipet aid (Powerpette; VWR, Radnor, PA). Solution replacements were not applied in either of the two control groups. At the end of the testing, each specimen was gently removed from the BioRakes and stored in a microcentrifuge tube filled with 37 °C HBSS prior to preparing samples for the collagen assay. Load values registered during stress relaxation were converted to engineering stresses based on sample dimensions, and the associated normalized stresses were calculated by dividing the engineering stress at each time point by the initial stress at t = 0.[47,48]

Collagen assay

Noncross-linked, fibrillar collagens were extracted from valvular tissue samples in an acetic acid–pepsin solution for 72 h, following which collagen concentrations were quantified via an assay kit (Sircol S1000; Accurate Chemical & Scientific Corp., Westbury, NY) per our previously published protocol.[40] Note that following biaxial stress relaxation studies, samples were rinsed thoroughly in HBSS to remove to the extent possible residual collagenase and/or collagen fragments, weighed, and immediately immersed into extraction solution. While only n = 3 AV and n = 3 PV leaflets were available for each condition, a total of n = 4 samples from each condition were selected for the collagen assays (i.e. two small samples were arbitrarily taken from one of the three leaflet samples) and weighed using an analytical balance (VWR).

AQ1

Statistics

For normalized stress at t = 10,000 s (i.e. a measure of the rate of stress relaxation) and collagen concentration, the two experimental factors (i.e. collagenase concentration and percentage equibiaxial strain) were analyzed independently by nonparametric Kruskal–Wallis tests. Of note, nonparametric statistics were utilized due to the relatively low sample numbers, thereby making no assumption regarding the normality of the distribution. For comparisons between the 37.5% and 50% equibiaxial strain groups at individual collagenase concentrations, Mann–Whitney tests (i.e. nonparametric t-tests) were conducted. Statistics were calculated using Prism 5 software (version 5.04; GraphPad Software, Inc., La Jolla, CA). For reference, data are also reported as mean ± standard error of the mean (SEM) for n = 3 (normalized stress at t = 10,000 s) and n = 4 (collagen concentration) samples in Tables 1 and 2, respectively.

Results

Normalized stress relaxation curves (mean ± SEM; n = 3) for AV and PV samples held at 50% equibiaxial strain are presented in Figure 1(a) and (b) and (c) and (d), respectively. Of note, normalized stress relaxation curves for samples held at 37.5% equibiaxial strain appeared qualitatively similar (data not shown).

Experimental tissues exhibited a discontinuity in stress relaxation response at t = 3000 s, synchronous with the exchange of HBSS for either 0.2 or 0.5 mg/mL collagenase solution. Of note, in some experimental samples, a small transient increase in load was observed at t = 3000 s, due to draining the BioTester fluid bath and associated loss of tissue buoyancy under the influence of gravity.

Qualitative inspection of the stress relaxation curves revealed gross evidence that experimental, collagenase-treated tissues relaxed more rapidly than control,

AQ2 **Table 1.** Normalized stress at t = 10,000 s (mean ± SEM, n = 3).

Valve, % strain, direction	Collagenase concentration (mg/mL)		
	0 (control)	0.2	0.5
AV, 37.5, circumferential	0.42 ± 0.01	0.17 ± 0.01	0.09 ± 0.01
AV, 37.5, radial	0.50 ± 0.01	0.20 ± 0.03	0.10 ± 0.01
AV, 50, circumferential	0.46 ± 0.01	0.13 ± 0.02	0.03 ± 0.02
AV, 50, radial	0.51 ± 0.01	0.13 ± 0.03	0.06 ± 0.02
PV, 37.5, circumferential	0.40 ± 0.07	0.12 ± 0.01	0.08 ± 0.04
PV, 37.5, radial	0.57 ± 0.03	0.13 ± 0.01	0.04 ± 0.04
PV, 50, circumferential	0.46 ± 0.03	0.14 ± 0.02	0.02 ± 0.01
PV, 50, radial	0.50 ± 0.03	0.10 ± 0.05	0.01 ± 0.01

Data are presented for aortic valve (AV) and pulmonary valve (PV) leaflet tissues under two different equibiaxial strain conditions and two different material directions (row labels: 37.5% and 50% strains and circumferential and radial directions) and three different collagenase concentration conditions (column labels: 0 (control), 0.2, and 0.5 mg/mL).

Table 2. Collagen concentration (μg/g wet weight; mean ± SEM, n = 4).

Valve, % strain	Collagenase concentration (mg/mL)		
	0 (control)	0.2	0.5
AV, 0 (control)	58000 ± 5700	56000 ± 1900	36000 ± 2500
AV, 37.5	56000 ± 4400	39000 ± 6400	18000 ± 1800
AV, 50	61000 ± 5500	40000 ± 5400	18000 ± 1400
PV, 0 (control)	81000 ± 7100	66000 ± 7400	46000 ± 4500
PV, 37.5	78000 ± 6100	49000 ± 5600	33000 ± 5000
PV, 50	81000 ± 8900	30000 ± 1800	18000 ± 1600

Data are presented for aortic valve (AV) and pulmonary valve (PV) leaflet tissues under three different equibiaxial strain conditions (row labels: 0% (control), 37.5%, and 50%) and three different collagenase concentration conditions (column labels: 0 (control), 0.2, and 0.5 mg/mL).
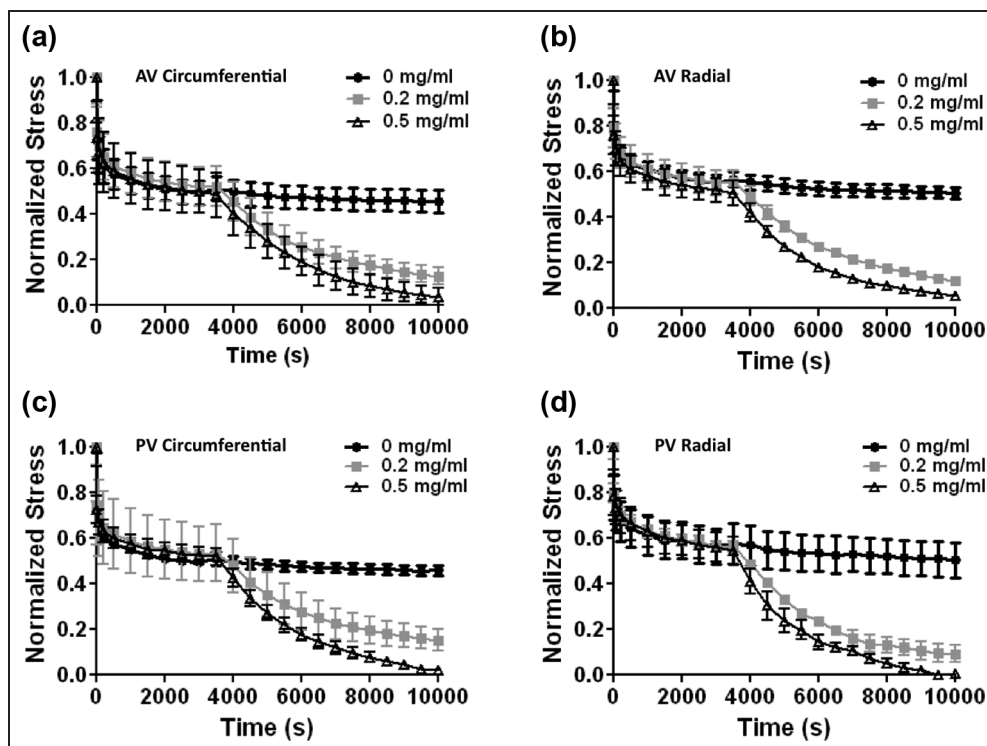

Figure 1. Normalized stress relaxation curves under 50% equibiaxial strain (mean ± SEM; n = 3): (a) aortic valve (AV) normalized circumferential stress, (b) AV normalized radial stress, (c) pulmonary valve (PV) normalized circumferential stress, and (d) PV normalized radial stress. For the collagenase-treated groups, Hank's balanced salt solution (HBSS) was replaced with 0.2 or 0.5 mg/mL collagenase solution after 3000 s; for the control group (i.e. 0 mg/mL), HBSS was not replaced.
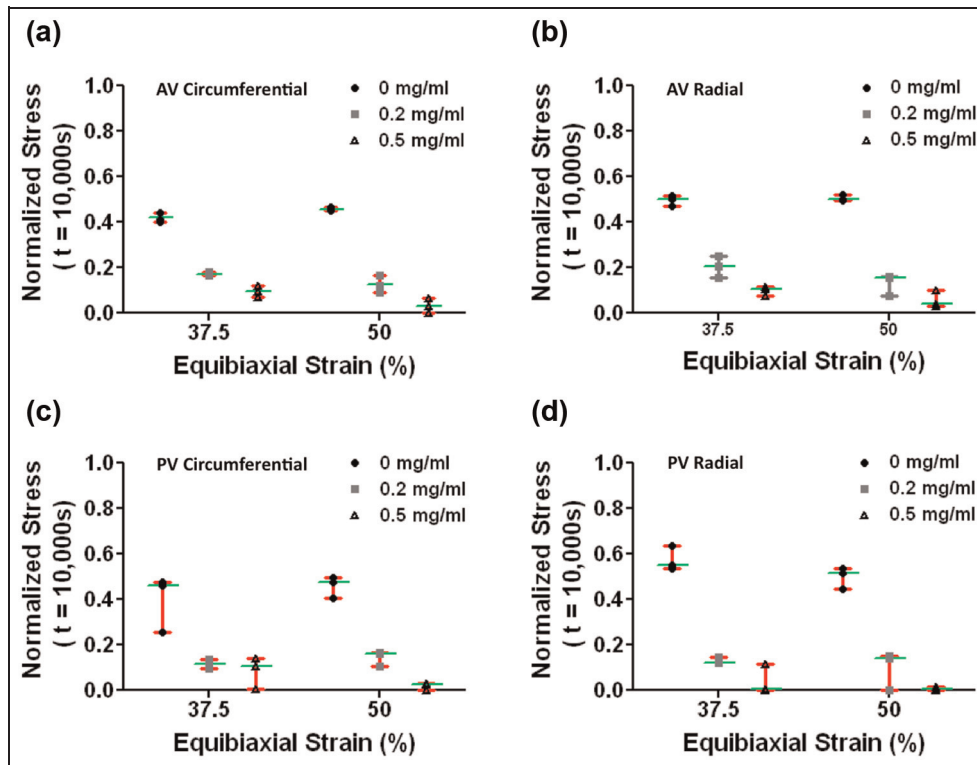
Figure 2. Normalized stresses at t = 10,000 s relaxation (n = 3 per group; medians and ranges are indicated by green lines and red error bars, respectively): (a) aortic valve (AV) normalized circumferential stress, (b) AV normalized radial stress, (c) pulmonary valve (PV) normalized circumferential stress, and (d) PV normalized radial stress. Kruskal–Wallis test p-values, indicating significant ($p < 0.05$) or nonsignificant (n.s.) differences, were calculated as follows: for (a), *effect of collagenase concentration at 37.5% strain* ($p = 0.0273$, *) and 50% strain ($p = 0.aa0273$, *); for (b), *effect of collagenase concentration at 37.5% strain* ($p = 0.0273$, *) and 50% strain ($p = 0.0390$, *); for (c), *effect of collagenase concentration at 37.5% strain* ($p = 0.0665$, n.s.) and 50% strain ($p = 0.0273$, *); and for (d), *effect of collagenase concentration at 37.5% strain* ($p = 0.0265$, *) and 50% strain ($p = 0.0509$, n.s.). Note that Mann–Whitney tests (i.e. nonparametric t-tests) conducted between strain levels at different collagenase concentrations were all nonsignificant.

untreated tissues (Figure 1(a)–(d)). Moreover, tissues treated with 0.5 mg/mL collagenase qualitatively appeared to relax more rapidly than those treated with 0.2 mg/mL collagenase. Potential differences associated with other factors, such as 37.5% versus 50% equibiaxial strain, circumferential versus radial loading axis, and AV versus PV, were not readily discernable by qualitative inspection of the stress relaxation curves. For the purpose of comparing experimental to control groups, the normalized stress (remaining) at t = 10,000 s was utilized as a single quantitative measure of the rate of stress relaxation within the range t = 3000 and 10,000 s.

Normalized stress measurements at t = 10,000 s (median and range; n = 3) are presented as dot plots in Figure 2, with associated nonparametric (Kruskal–Wallis) statistics indicated below and in the associated figure caption. For reference, data are also tabulated as mean ± SEM in Table 1 (not for statistical comparisons, due to relatively low sample numbers). In the AV, increasing the collagenase concentration significantly accelerated the rate of stress relaxation in the circumferential direction at 37.5% ($p = 0.0273$) and 50% ($p = 0.0273$) strain (Figure 2(a)), as well as in the radial

direction at 37.5% ($p = 0.0273$) and 50% ($p = 0.0390$) strain (Figure 2(b)). In the PV, the effect of increasing the collagenase concentration on the rate of stress relaxation did not reach statistical significance in the circumferential direction at 37.5% strain ($p = 0.0665$) but was found to be significant at 50% strain ($p = 0.0273$; Figure 2(c)). In the PV radial direction, increasing the collagenase concentration significantly accelerated the rate of stress relaxation at 37.5% strain ($p = 0.0273$), but did not reach significance at 50% strain ($p = 0.0509$; Figure 2(d)).

In the AV and PV, any potential effects of equibiaxial strain magnitude (i.e. 50% vs 37.5%) on the rate of stress relaxation were less pronounced in the context of the relatively small n = 3 samples per group. In the AV circumferential and radial directions, there appeared to be a trend of decreased normalized stress with increased equibiaxial strain magnitude; however, comparisons failed to reach statistical significance by Mann–Whitney tests (i.e. nonparametric t-tests) between 37.5% and 50% strain groups in all of the individual collagenase concentration groups (i.e. 0, 0.2, and 0.5 mg/mL; Figure 2). No similar trends were readily apparent in the case of the PV.
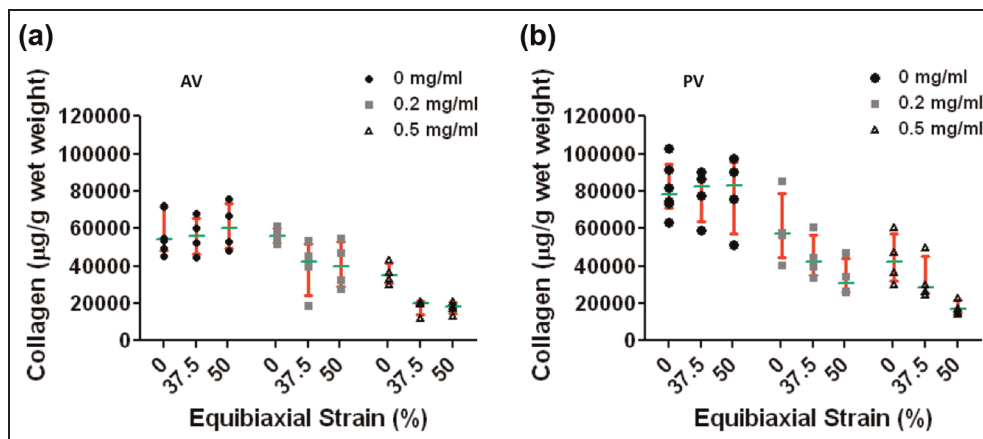
Figure 3. Collagen concentrations measured for (a) AV and (b) PV samples (n = 4 per group; medians and interquartile ranges are indicated by green lines and red error bars, respectively). Kruskal–Wallis test *p*-values, indicating significant ($p < 0.05$, *; $p < 0.01$, **) or nonsignificant (n.s.) differences, were calculated as follows: for (a), *effect of equibiaxial strain* in the absence of collagenase ($p = 0.8325$, n.s.), at 0.2 mg/mL collagenase ($p = 0.0837$, n.s.), and at 0.5 mg/mL collagenase ($p = 0.0231$, *); *effect of collagenase concentration* in the absence of strain ($p = 0.0181$, *), at 37.5% strain ($p = 0.0388$, *), and at 50% strain ($p = 0.0125$, *); for (b), *effect of equibiaxial strain* in the absence of collagenase ($p = 0.9603$, n.s.), at 0.2 mg/mL collagenase ($p = 0.0976$, n.s.), and at 0.5 mg/mL collagenase ($p = 0.0183$, *); *effect of collagenase concentration* in the absence of strain ($p = 0.0213$, *), at 37.5% strain ($p = 0.0218$, *), and at 50% strain ($p = 0.0073$, **).

Collagen concentration measurements (median ± interquartile range; n = 4) are presented as dot plots in Figure 3, with associated nonparametric (Kruskal–Wallis) statistics indicated below and in the associated figure caption. For reference, data are also tabulated as mean ± SEM in Table 2 (not for statistical comparisons, due to relatively low sample numbers). In the AV, increasing the collagenase concentration led to significantly lower collagen concentrations in the absence of strain (0% strain; $p = 0.0181$), at 37.5% strain ($p = 0.0388$), and at 50% strain ($p = 0.0125$; Figure 3(a)). Similarly, in the PV, increasing the collagenase concentration led to significantly lower collagen concentrations in the absence of strain (0% strain; $p = 0.0213$), at 37.5% strain ($p = 0.0218$), and at 50% strain ($p = 0.0073$; Figure 3(b)).

In the AV and PV, any potential effects of equibiaxial strain magnitude (i.e. 50% vs 37.5%) on collagen concentration were less pronounced in the context of the relatively small n = 3 samples per group. In the AV, equibiaxial strain showed no significant effect in the absence of collagenase ($p = 0.8325$) or at 0.2 mg/mL collagenase ($p = 0.0837$); by contrast, increasing equibiaxial strain led to a significantly lower collagen concentration at 0.5 mg/mL collagenase ($p = 0.0231$; Figure 3(a)). Similarly, in the PV, equibiaxial strain showed no significant effect in the absence of collagenase ($p = 0.9603$) or at 0.2 mg/mL collagenase (0.0976); by contrast, increasing equibiaxial strain led to a significantly lower collagen concentration at 0.5 mg/mL collagenase ($p = 0.0183$; Figure 3(b)).

Qualitatively, while AV tissues exhibited lower collagen concentrations following stress relaxation under 37.5% and 50% equibiaxial strain (relative to the control, 0% strain condition), the effect appeared to

saturate, with collagen concentrations at 50% equibiaxial strain appearing to be indistinguishable from those at 37.5% strain (Figure 3(a)). Notably, this behavior appeared to be consistent across 0.2 and 0.5 mg/mL collagenase concentration conditions. By contrast, in the PV tissues, collagen concentration appeared to continue decreasing on going from 37.5% to 50% equibiaxial strain, consistently across 0.2 and 0.5 mg/mL collagenase concentration conditions (Figure 3(b)).

Discussion

Collagen is at the heart of any and all questions concerning semilunar valvular leaflet composition, structure, and function. Whether during development, physiological homeostasis, or pathological degeneration, it is the structural–mechanical state of the heart valve leaflet collagen network that ultimately confers valvular function and the difference between health and disease.[49] While MMP-mediated collagen remodeling is recognized as a key aspect of valvular physiology and pathology[22,23] and plays a significant role in bioprosthetic heart valve degeneration,[50,51] it remains unclear how MMPs are capable of differentiating between damaged and undamaged collagen fibers once unleashed by VICs, selectively degrading damaged collagen fibers and leaving undamaged, structurally load-bearing fibers unscathed.

Since the seminal work of Huang and Yannas,[29] it has been appreciated that the susceptibility of collagen to enzymatic cleavage can depend on the strain state of the fiber. While protective[29,30] and accelerative effects[41,52] have since been shown in tissues ranging from tendon[29,30,52] to pericardium,[41] to the best of the

authors' knowledge, this study is the first to investigate such phenomena in the context of valvular tissues.

Collagen concentration measurements

Collagen concentrations measured for control porcine AV and PV leaflets were not significantly different than those previously reported by our group.[40] For comparison, Schenke-Layland et al.[21] recently reported similar order of magnitude of collagen concentrations for control porcine AV leaflets, as measured using the same Sircol collagen assay kit and an unspecified extraction protocol (34,500 ± 1600 μg/g wet weight). Control porcine PV collagen concentrations measured in our current and previous studies (~60,000 μg/g wet weight) were about twofold higher than those reported by Schenke-Layland et al.,[21] potentially associated with our 72-h digestion protocol, which is longer than previously reported 16-h extraction times applied to engineered heart valve tissues[53,54] and which could potentially have been longer than those utilized by Schenke-Layland et al.[21] In the context of native heart valve leaflets, we previously demonstrated that 72-h acetic acid–pepsin extraction yielded a stable plateau value of collagen concentration as a function of digestion time.[40]

In interpreting collagen concentration measurements, it is important to note the following factors. First, bacterial collagenase breaks down collagen into fragments that are not detectable by the Sircol assay, cleaving at X-Gly-Pro-Y sites and yielding about 200 cleavages per alpha chain.[55] This suggests that collagen catabolized during bacterial collagenase incubation should not contribute to the collagen concentration measured by subsequent acetic acid–pepsin-based digestion of the remaining collagen. Second, while bacterial collagenase (and endogenous MMPs) can digest covalently cross-linked collagen, the acetic acid–pepsin solublization protocol used in conjunction with the standard (S1000) Sircol collagen assay kit is not designed to release covalently cross-linked collagens. Thus, in considering potential effects of collagenase and strain state on the residual collagen concentration remaining within the valvular tissue, it must be kept in mind that the various subpopulations of collagen, including immature, noncross-linked collagens and mature, cross-linked collagens, may both contribute to the load-bearing capacity of the tissue but may be differentially affected by collagenase treatment.

Recently, a new Sircol insoluble collagen assay kit (S2000) was released by Biocolor Ltd (Carrickfergus, Northern Ireland, United Kingdom) for the purpose of extracting and assaying insoluble collagens, which previously required measurement by hydroxyproline assay. In light of differences in the collagen remodeling potential and stiffness of pulmonary valvular interstitial cell (PVICs) versus aortic valvular interstitial cell (AVICs),[14] as well as PV versus AV differences in heat shock protein (HSP)-47 expression, an indicator of collagen synthesis,[1] it will be informative in future studies to measure the ratios of soluble to insoluble collagen in the AV and PV. In particular, the higher acid–pepsin soluble collagen concentration measured for the PV here and in our previous study[40] could potentially reflect a larger ratio of soluble to insoluble collagen in the PV versus AV, rather than a higher total collagen concentration. This possibility is supported by Aldous et al.,[7] who demonstrated that the collagen of the bovine AV contains a greater number of mature histidinohydroxylysinonorleucine (HHL) cross-links than that of the PV, suggesting that the AV could exhibit a lower ratio of soluble to insoluble collagen, potentially manifesting as a lower apparent collagen concentration than the PV, in the case that only the acid–pepsin soluble fraction of the total collagen is considered.

Normalized stress measurements

Equibiaxial stress relaxation results presented herein for AV and PV leaflet tissues in the circumferential and radial directions are consistent with uniaxial results of Huang and Yannas[29] with regard to the effects of collagenase concentration, with increased collagenase concentration yielding increased rates of stress relaxation, as demonstrated herein by significant decreases in the normalized stress (remaining) at 10,000 s in the collagenase-treated versus untreated control groups (Figure 2(a)–(d)).

In contrast to the protective effect of 4% strain Huang and Yannas[29] demonstrated in the context of a collagenase-mediated catabolism of a bovine tendon-derived collagen tape, here we observed what appeared to be an accelerative effect, although it did not reach statistical significance. In particular, there appeared to be a trend of lower normalized stress (remaining) at 10,000 s in the 50% versus 37.5% AV circumferential and AV radial groups. Given the small (n = 3) sample size, further testing may strengthen the observed trend. Results for the PV did not indicate any significant differences or obvious trends in association with strain magnitude. The apparent difference in the behavior of the PV versus the AV may be related to differences in their respective collagen fiber network architectures (i.e. collagen fiber orientation distributions). Indeed, Joyce et al.[56] demonstrated significant differences between the PV and AV collagen fiber orientation distribution, with the PV exhibiting a greater degree of uniformity than the AV, which could have implications not only for the stress relaxation behaviors observed herein but also for the potentially strain-dependent capacity of the PV collagen fiber network to adapt to the higher pressure, higher strain environment of the AV position in the Ross procedure.[57]

Given the high degree of anisotropy exhibited by AV and PV leaflet tissues, it is important to also consider how collagen fiber angular orientations may change during loading. Billiar and Sacks[58] were the first to experimentally demonstrate shifts in the centroid and

breadth of the AV collagen fiber orientation distribution under biaxial strain. In particular, they demonstrated that a stretch of 4% along the preferred (i.e. circumferential) direction (held to initial length in radial direction) yielded a decrease in the already narrow collagen fiber orientation distribution centered about the circumferential loading axis. By contrast, a stretch to 70% strain along the cross-preferred (i.e. radial) direction (held to initial length in circumferential direction) yielded a relatively subtle broadening of the collagen fiber orientation distribution, indicative of some fibers rotating toward the radial loading axis.[58]

While distinct from the 1:1 equibiaxial strains imposed in this study, the results of Billiar and Sacks demonstrate that not only the initial collagen fiber orientation but also the fiber rotations under loading must be considered in evaluating the effects of strain state on collagen susceptibility to proteolysis. More recently, Aggarwal et al.[59] demonstrated significant differences between normal, tricuspid AV and bicuspid AV collagen fiber orientation distributions, with the bicuspid AV exhibiting, on average, a disorganized, relatively unaligned belly region compared with the normal, tricuspid AV. In light of the fact that bicuspid AV often progresses to AV calcification, these findings suggest that the susceptibility to collagen catabolism may vary regionally in different leaflets and leaflet disease states, potentially promoting disease progression. Such possibilities are supported by observations of higher MMP expression in the direct vicinity of calcific nodules in valve tissues,[24] demonstration by Fisher et al.[60] that VIC calcification in vitro is strain dependent, and may elicit up to twofold strain amplification adjacent calcific nodules.

Effects of strain state on collagen catabolism

This study focused exclusively on native porcine AVs and PVs and investigated collagen catabolism during stress relaxation under a limited subset of potentially relevant equibiaxial strain states (i.e. 37.5% and 50%). These relatively large strains were chosen such as to promote uncrimping and rotation of valvular collagen fibers into the orthogonal directions of loading, thereby maximizing the tensile strain experienced by individual fibers and offering the opportunity to observe for potential effects at the high end of the valvular stress–strain range. However, in contrast to Huang and Yannas[29] and Nabeshima et al.,[30] who observed a protective effect of 4% strain in the context of a bovine tendon-derived collagen tape[29] and native rabbit patellar tendon,[30] respectively, the application of relatively large strains to porcine AV and PV in this study appeared to have the opposite effect, increasing the rate of collagenolysis.

Ruberti and Hallab[38] were the first to conclusively demonstrate selective proteolysis of unstrained collagen fibers, leveraging the orthogonal collagen fiber orientations intrinsic to corneal tissue to provide an internal control to their study, thereby mitigating the possibility of diffusional differences between strained and unstrained tissues confounding results. Specifically, bovine corneal tissues were loaded uniaxially to approximately 10–20 times physiological load (i.e. 15–30 pN force per collagen molecule), and time-lapse polarized light microscopy was utilized to track changes in collagen birefringence, which initially comprised contributions from both axes. Loaded and unloaded samples were exposed to 0.1 mg/mL bacterial collagenase and followed for up to 120 h (i.e. 432,000 s), during which time significant changes in birefringence were evident, with the component associated with the unloaded axis progressively diminishing with time. Results were confirmed by polarized light microscopy of fixed tissues and transmission electron microscopy, which demonstrated direct evidence of selective degradation of unloaded fibers.

Building upon this seminal study, Ruberti and colleagues[33,37,38] published a number of studies demonstrating further evidence for collagen's strain-dependent susceptibility to proteolysis, utilizing their unique "internally controlled" corneal tissue model, as well as via a variety of elegant single fiber[34] and reconstituted collagen gel-based models[31,36] designed to eliminate potentially confounding factors associated with native tissues, such as the presence of cross-linking, proteoglycans. In addition to direct effects of strain state on collagen molecules, strain is known to exert significant effects on the expression of collagenolytic MMPs and cathepsins in valvular tissues.[22,23]

Toward elucidating the role of pathologically altered mechanical environments in mediating valvular MMP expression, Balachandran et al.[22] subjected native porcine AV samples to in vitro cyclic stretch for periods of 24–48 h (10%, 15%, and 20% uniaxial tensile strain in the circumferential direction, approximating physiological, hypertensive, and severely hypertensive strains, respectively; 1.167 Hz, i.e., 70 beats/min). Elevated cyclic stretch was demonstrated to be capable of eliciting significant increases in MMP-1, -2, and -9, paralleled by significant decreases in tissue inhibitor of metalloproteinase (TIMP)-1 expression.[22] Interestingly, in addition to observations regarding MMP expression, Balachandran et al. reported significant increases in the collagen concentration measured with elevated (15% and 20%) cyclic strain and a significant decrease with approximately physiologic (10%) cyclic strain, relative to fresh controls. Collagen was extracted using pepsin and assayed utilizing the same Sircol collagen assay utilized in this study, only with a significantly shorter, 24 h, extraction time. A highly plausible explanation put forth by Balachandran et al. was that the VICs present within the AV samples upregulated collagen production in response to the higher, 15%–20%, levels of cyclic stretch. An alternative and/or complementary explanation, however, could be that the pathological magnitudes of cyclic strain may have rendered the original valvular collagen more susceptible to proteolysis

by the expressed MMPs. By contrast, cyclic stretch mimicking physiological strain amplitude (i.e. 10%) may have exerted a protective effect relative to fresh tissue, thereby yielding the appearance of a lower collagen content in the 10% strain group. While this alternative or complementary explanation is necessarily speculative, these observations provide a basis for future experimental designs.

Limitations of this study

Limitations of this study include the relatively small (n = 3 or 4) number of samples tested per group, potential species differences (i.e. porcine vs human[61]), and the limited range of strains tested (i.e. 37.5% and 50% equibiaxial strain). Huang and Yannas[29] demonstrated significant effects of uniaxial tensile strain on the collagenase sensitivity of a cross-linked, collagen-based surgical tape, within the strain range of 1%–7%, with a minimum rate of collagenase degradation observed at 4% strain. In the case of the bovine tendon-derived collagen surgical tape (Ethicon, Inc., Bridgewater, NJ), the minimum rate of collagenase-mediated collagen degradation appeared to coincide with the inflection point of the stress–strain curve, where the uncrimping of collagen fibers in the toe region is largely complete, giving way to an abrupt rise in stress as straightened collagen fibers are fully loaded under tension.[29]

Huang and Yannas speculated that the decreased rate of collagenase-mediated collagen degradation observed under low (1%–4%) strain may have been related to reduced collagenase flux into the tissue at these low strains, associated with the crimped collagen structure. As highlighted in recent work by Ruberti's group, Huang and Yannas[29] speculated that the increased rate of collagenase-mediated collagen degradation at higher strains could have derived from one or a combination of mechanisms, including that hypothesized by Ruberti and colleagues,[32,34] an "opening" of enzymatic sites to attack, due to strain-mediated changes in the collagen molecule's three-dimensional configuration: a "mechanochemical switch." How the inflection point of the stress–strain curve may relate to sensitivity of semilunar heart valve collagen susceptibility to proteolysis remains unclear, as this study only assessed the effects of 37.5% and 50% strain, which are both well within the exponential portion of the stress–strain responses, in the radial and circumferential directions. Huang et al.[10] previously demonstrated experimentally and computationally how VICs deform in response to strain magnitude, approaches which may be useful in interpreting future studies conducted under different strains.

AQ3

In future studies, it will be important to assess the effects of a broader range of strains bracketing the inflection point, which corresponds with approximately 20%–25% in the circumferential direction.[40] The 37.5%–50% strain range investigated in this study does bracket the inflection point of native AV and PV tissues

in the radial direction, which occurs at approximately 35% strain under equibiaxial strain.[40] As indicated above, depending on the strain range and the tissue in question, studies have demonstrated evidence that strain state can serve as either a protective[30] or accelerative[41,52] factor in collagen catabolism. While this study is thought to be the first to evaluate potential effects of biaxial strain state on the susceptibility of native valvular collagens to proteolysis, a previous study by Ellsmere et al.[41] demonstrated that cyclic mechanical loading and associated fatigue damage can increase the collagenase susceptibility of bovine pericardium, a tissue routinely utilized in fabricating chemically fixed bioprosthetic heart valves.

Related to the range of strains explored, another limitation of this study is its emphasis on only equibiaxial strains. As indicated in the methods, equibiaxial strain was utilized here because equibiaxial strain minimizes collagen fiber rotations, largely preserving the original collagen fiber orientations.[43] As a result, tissue-level strains (e.g. 37.5% and 50%) would be expected to be more effectively transferred to the collagen fibers. However, the strains experienced by AV leaflets during diastole (i.e. when the valve is closed) differ in the circumferential and radial directions, reaching ~15% to as high as ~80%, respectively.[62,63] In future studies, it will be important to investigate other, more physiological biaxial loading protocols.

Conclusion

In their seminal 1977 article, Huang and Yannas[29] set the stage for a new paradigm of collagen fiber remodeling, one in which the strain state of individual collagen fibers is capable of influencing their own susceptibility to proteolysis. Since protective[29,30] and accelerative effects[41,52] of collagen strain state have been demonstrated in tissues including tendon and tendon-derived materials,[29,30,52] pericardium,[41] cornea,[33,37,38] and reconstituted collagen networks.[31,36] To the best of the authors' knowledge, this study is the first to investigate such phenomena in the context of valvular tissues. Herein, we demonstrated that at a collagenase concentration of 0.5 mg/mL, increasing the equibiaxial strain imposed during stress relaxation yielded significantly lower median collagen concentrations in the AV and PV, paralleled by trends of accelerated normalized stress relaxation rate with equibiaxial strain in AV tissues. Collectively, these in vitro results indicate that biaxial strain state is capable of affecting the susceptibility of valvular collagens to catabolism, providing a basis for further investigation of how such phenomena may manifest at different strain magnitudes or in vivo.

AQ4

AQ5

References

1. Merryman WD, et al. Correlation between heart valve interstitial cell stiffness and transvalvular pressure: implications for collagen biosynthesis. *Am J Physiol Heart Circ Physiol* 2006; 290(1): H224–H231.
2. Corden J, David T and Fisher J. Determination of the curvatures and bending strains in open trileaflet heart valves. *Proc IMechE, Part H: J Engineering in Medicine* 1995; 209(2): 121–128.
3. Iyengar AKS, et al. Dynamic in vitro quantification of bioprosthetic heart valve leaflet motion using structured light projection. *Ann Biomed Eng* 2001; 29(11): 963–973.
4. Sugimoto H and Sacks MS. Effects of leaflet stiffness on dynamic bioprosthetic heart valve leaflet shape. *Cardiovasc Eng Technol* 2013; 4(1): 2–15.
5. Yap CH, et al. Experimental measurement of dynamic fluid shear stress on the aortic surface of the aortic valve leaflet. *Biomech Model Mechanobiol* 2012; 11(1–2): 171–182.
6. Weston MW, LaBorde DV and Yoganathan AP. Estimation of the shear stress on the surface of an aortic valve leaflet. *Ann Biomed Eng* 1999; 27(4): 572–579.
7. Aldous IG, et al. Differences in collagen cross-linking between the four valves of the bovine heart: a possible role in adaptation to mechanical fatigue. *Am J Physiol Heart Circ Physiol* 2009; 296(6): H1898–H1906.
8. Van der Kamp AW and Nauta J. Fibroblast function and the maintenance of the aortic-valve matrix. *Cardiovasc Res* 1979; 13(3): 167–172.
9. Sacks MS, et al. Bioprosthetic heart valve heterograft biomaterials: structure, mechanical behavior and computational simulation. *Expert Rev Med Devices* 2006; 3(6): 817–834.
10. Huang HY, Liao J and Sacks MS. In-situ deformation of the aortic valve interstitial cell nucleus under diastolic loading. *J Biomech Eng* 2007; 129(6): 880–889.
11. Lewinsohn AD, et al. Anisotropic strain transfer through the aortic valve and its relevance to the cellular mechanical environment. *Proc IMechE, Part H: J Engineering in Medicine* 2011; 225(8): 821–830.
12. Merryman WD, et al. Synergistic effects of cyclic tension and transforming growth factor-beta1 on the aortic valve myofibroblast. *Cardiovasc Pathol* 2007; 16(5): 268–276.
13. Rabkin-Aikawa E, et al. Dynamic and reversible changes of interstitial cell phenotype during remodeling of cardiac valves. *J Heart Valve Dis* 2004; 13(5): 841–847.
14. Merryman WD, et al. Differences in tissue-remodeling potential of aortic and pulmonary heart valve interstitial cells. *Tissue Eng* 2007; 13(9): 2281–2289.
15. Rabkin E, et al. Activated interstitial myofibroblasts express catabolic enzymes and mediate matrix remodeling in myxomatous heart valves. *Circulation* 2001; 104(21): 2525–2532.
16. Sacks MS and Schoen FJ. Collagen fiber disruption occurs independent of calcification in clinically explanted bioprosthetic heart valves. *J Biomed Mater Res* 2002; 62(3): 359–371.
17. Banerjee T, et al. Clinical significance of markers of collagen metabolism in rheumatic mitral valve disease. *PLoS ONE* 2014; 9(3): e90527.
18. Lacerda CM, et al. Static and cyclic tensile strain induce myxomatous effector proteins and serotonin in canine mitral valves. *J Vet Cardiol* 2012; 14(1): 223–230.
19. Cole WG, et al. Collagen composition of normal and myxomatous human mitral heart valves. *Biochem J* 1984; 219(2): 451–460.
20. Quick DW, et al. Collagen synthesis is upregulated in mitral valves subjected to altered stress. *ASAIO J* 1997; 43(3): 181–186.
21. Schenke-Layland K, et al. Cardiomyopathy is associated with structural remodelling of heart valve extracellular matrix. *Eur Heart J* 2009; 30(18): 2254–2265.
22. Balachandran K, et al. Elevated cyclic stretch alters matrix remodeling in aortic valve cusps: implications for degenerative aortic valve disease. *Am J Physiol Heart Circ Physiol* 2009; 296(3): H756–H764.
23. Fondard O, et al. Extracellular matrix remodelling in human aortic valve disease: the role of matrix metalloproteinases and their tissue inhibitors. *Eur Heart J* 2005; 26(13): 1333–1341.
24. Perrotta I, et al. Matrix metalloproteinase-9 expression in calcified human aortic valves: a histopathologic, immunohistochemical, and ultrastructural study. *Appl Immunohistochem Mol Morphol.* Epub ahead of print 11 November 2014. DOI: 10.1097/PAI.0000000000000144.
25. Huang S and Huang HY. Prediction of matrix-to-cell stress transfer in heart valve tissues. *J Biol Phys* 2015; 41: 9–22.
26. Huang S and Huang HY. Virtualisation of stress distribution in heart valve tissue. *Comput Methods Biomech Biomed Engin* 2014; 17: 1696–1704.
27. Carruthers CA, et al. Gene expression and collagen fiber micromechanical interactions of the semilunar heart valve interstitial cell. *Cell Mol Bioeng* 2012; 5(3): 254–265.
28. Anssari-Benam A, Gupta HS and Screen HR. Strain transfer through the aortic valve. *J Biomech Eng* 2012; 134(6): 061003.
29. Huang C and Yannas IV. Mechanochemical studies of enzymatic degradation of insoluble collagen fibers. *J Biomed Mater Res* 1977; 11(1): 137–154.
30. Nabeshima Y, et al. Uniaxial tension inhibits tendon collagen degradation by collagenase in vitro. *J Orthop Res* 1996; 14(1): 123–130.
31. Bhole AP, et al. Mechanical strain enhances survivability of collagen micronetworks in the presence of collagenase: implications for load-bearing matrix growth and stability. *Philos Trans A Math Phys Eng Sci* 2009: 367(1902): 3339–3362.
32. Camp RJ, et al. Molecular mechanochemistry: low force switch slows enzymatic cleavage of human type I collagen monomer. *J Am Chem Soc* 2011; 133(11): 4073–4078.
33. Robitaille MC, et al. Small-angle light scattering to detect strain-directed collagen degradation in native tissue. *Interface Focus* 2011; 1(5): 767–776.
34. Flynn BP, Tilburey GE and Ruberti JW. Highly sensitive single-fibril erosion assay demonstrates mechanochemical

switch in native collagen fibrils. *Biomech Model Mechano-biol* 2013; 12(2): 291–300.

35. Chang SW, et al. Molecular mechanism of force induced stabilization of collagen against enzymatic breakdown. *Biomaterials* 2012; 33(15): 3852–3859.

36. Flynn BP, et al. Mechanical strain stabilizes reconstituted collagen fibrils against enzymatic degradation by mammalian collagenase matrix metalloproteinase 8 (MMP-8). *PLoS ONE* 2010; 5(8): e12337.

37. Zareian R, et al. Probing collagen/enzyme mechanochemistry in native tissue with dynamic, enzyme-induced creep. *Langmuir* 2010; 26(12): 9917–9926.

38. Ruberti JW and Hallab NJ. Strain-controlled enzymatic cleavage of collagen in loaded matrix. *Biochem Biophys Res Commun* 2005; 336(2): 483–489.

39. Sacks MS, Smith DB and Hiester ED. A small angle light scattering device for planar connective tissue microstructural analysis. *Ann Biomed Eng* 1997; 25(4): 678–689.

40. Huang HY, Balhouse BN and Huang S. Application of simple biomechanical and biochemical tests to heart valve leaflets: implications for heart valve characterization and tissue engineering. *Proc IMechE, Part H: J Engineering in Medicine* 2012; 226(11): 868–876.

41. Ellsmere JC, Khanna RA and Lee JM. Mechanical loading of bovine pericardium accelerates enzymatic degradation. *Biomaterials* 1999; 20(12): 1143–1150.

42. Rodriguez KJ and Masters KS. Regulation of valvular interstitial cell calcification by components of the extracellular matrix. *J Biomed Mater Res A* 2009; 90(4): 1043–1053.

43. Liao J, et al. Molecular orientation of collagen in intact planar connective tissues under biaxial stretch. *Acta Biomater* 2005; 1(1): 45–54.

44. Duncan AC, Boughner D and Vesely I. Dynamic glutaraldehyde fixation of a porcine aortic valve xenograft. I. Effect of fixation conditions on the final tissue viscoelastic properties. *Biomaterials* 1996; 17(19): 1849–1856.

45. Stella JA, Liao J and Sacks MS. Time-dependent biaxial mechanical behavior of the aortic heart valve leaflet. *J Biomech* 2007; 40(14): 3169–3177.

46. Grashow JS, et al. Planar biaxial creep and stress relaxation of the mitral valve anterior leaflet. *Ann Biomed Eng* 2006; 34(10): 1509–1518.

47. Anssari-Benam A, Bader DL and Screen HR. Anisotropic time-dependant behaviour of the aortic valve. *J Mech Behav Biomed Mater* 2011; 4(8): 1603–1610.

48. Becker WR and De Vita R. Biaxial mechanical properties of swine uterosacral and cardinal ligaments. *Biomech Model Mechanobiol* 2015; 14: 549–560.

49. Chester AH, et al. The living aortic valve: from molecules to function. *Glob Cardiol Sci Pract* 2014; 2014(1): 52–77.

50. Bracher M, et al. Matrix metalloproteinases and tissue valve degeneration. *J Long Term Eff Med Implants* 2001; 11(3–4): 221–230.

51. Simionescu DT, Lovekamp JJ and Vyavahare NR. Extracellular matrix degrading enzymes are active in porcine stentless aortic bioprosthetic heart valves. *J Biomed Mater Res A* 2003; 66(4): 755–763.

52. Willett TL, et al. Increased proteolysis of collagen in an in vitro tensile overload tendon model. *Ann Biomed Eng* 2007; 35(11): 1961–1972.

53. Engelmayr GC Jr, et al. The independent role of cyclic flexure in the early in vitro development of an engineered heart valve tissue. *Biomaterials* 2005; 26(2): 175–187.

54. Engelmayr GC Jr, et al. Cyclic flexure and laminar flow synergistically accelerate mesenchymal stem cell-mediated engineered tissue formation: implications for engineered heart valve tissues. *Biomaterials* 2006; 27(36): 6083–6095.

55. Han S, Blumenfeld OO and Seifter S. Specific identification of collagens and their fragments by clostridial and anti-collagenase antibody. *Anal Biochem* 1992; 201(2): 336–342.

56. Joyce EM, et al. Functional collagen fiber architecture of the pulmonary heart valve cusp. *Ann Thorac Surg* 2009; 87(4): 1240–1249.

57. Rabkin-Aikawa E, et al. Clinical pulmonary autograft valves: pathologic evidence of adaptive remodeling in the aortic site. *J Thorac Cardiovasc Surg* 2004; 128(4): 552–561.

58. Billiar KL and Sacks MS. A method to quantify the fiber kinematics of planar tissues under biaxial stretch. *J Biomech* 1997; 30(7): 753–756.

59. Aggarwal A, et al. Architectural trends in the human normal and bicuspid aortic valve leaflet and its relevance to valve disease. *Ann Biomed Eng* 2014; 42(5): 986–998.

60. Fisher CI, Chen J and Merryman WD. Calcific nodule morphogenesis by heart valve interstitial cells is strain dependent. *Biomech Model Mechanobiol* 2013; 12: 5–17.

61. Mavrilas D and Missirlis Y. An approach to the optimization of preparation of bioprosthetic heart valves. *J Biomech* 1991; 24(5): 331–339.

62. Yap CH, et al. Dynamic deformation characteristics of porcine aortic valve leaflet under normal and hypertensive conditions. *Am J Physiol Heart Circ Physiol* 2010; 298(2): H395–H405.

63. Christie GW and Barratt-Boyes BG. Age-dependent changes in the radial stretch of human aortic valve leaflets determined by biaxial testing. *Ann Thorac Surg* 1995; 60(2 Suppl.): S156–S158; discussion S159.